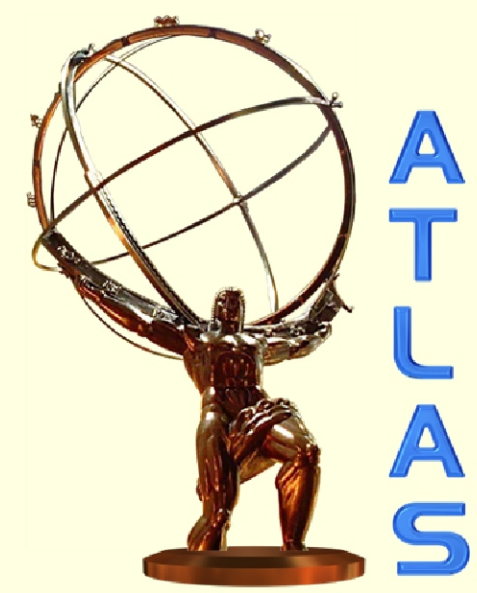


Operation of the ATLAS end-cap calorimeters at sLHC luminosities: an experimental study



For the ATLAS Liquid Argon HiLum group
Yuriy Tikhonov, Budker INP, Novosibirsk

The expected increase of luminosity at sLHC by a factor of ten with respect to LHC luminosities has serious consequences for the signal reconstruction, radiation hardness requirements and operations of the ATLAS liquid argon calorimeters (EMEC, HEC, FCAL) in the endcap, respectively forward region. Small modules of each type of calorimeter have been built and exposed to a high intensity proton beam of 60 GeV at IHEP (Protvino). The beam is extracted via the bent crystal technique, offering the unique opportunity to cover intensities ranging from 10^5 up to 10^{12} protons per second (pps). This exceeds the power density expected at sLHC by more than a factor of 100. In addition, the machine has been operated with the full RF bunch structure preserved and with 5-6 empty bunches between filled bunches. Thus the gap between two filled bunches was about 1 microsecond. This operation mode enables to study the high flux response of the calorimeters unaffected by pile-up and to reconstruct a clean signal over the full drift time of electrons in the liquid argon gap. The correlation between beam intensity and the read-out signal has been studied. Also the dependence of the HV currents as well as calorimeter module temperature on the beam intensity has been measured.

Introduction

The ATLAS Endcap calorimetry will be used to measure particle energy in the rapidity range from 1.5 to 4.9. It consists of the electromagnetic (EMEC), hadronic (HEC) and forward (FCAL) calorimeters with different electrode geometries (tube in FCAL, accordion in EMEC, and planar with electrostatic transformer in HEC). The calorimeters are designed to operate at the LHC luminosity of 10^{34} $\text{cm}^{-2}\text{s}^{-1}$. At this luminosity the maximum charged particle flux density is equal to $\sim 10^7$ ($\eta=5.0$) and $\sim 10^6$ ($\eta=3.2$) particles/s $\cdot\text{cm}^2$ for FCAL and EMEC/HEC, respectively (ATLAS calorimeter performance TDR, CERN/LHCC 96-40, 1996). The neutral particle flux is expected to be 10-20% higher. In a bin of $\Delta\eta \times \Delta\phi = 0.1 \times 0.1$ this corresponds to typically 10^{15} particles for 10 years of LHC or equivalently to an integrated energy of $6 \cdot 10^{15}$ GeV ($\eta=3.2$) or $28 \cdot 10^{15}$ GeV ($\eta=5.0$) respectively. These flux densities are several orders of magnitude higher than that in the presently operating liquid argon calorimeters. The particle flux densities will be in the range of $10^7 - 10^8$ particle/s $\cdot\text{cm}^2$ at the sLHC luminosity of 10^{35} $\text{cm}^{-2}\text{s}^{-1}$. Since the calorimeters will play a crucial role in the ATLAS research program it is very important to perform systematic studies of their characteristics at these huge particle fluxes. It was never done before for the realistic geometry of FCAL, EMEC and HEC electrodes.

The main goal of the present project is to establish the operating limits of the ATLAS endcap calorimeters in conditions as close as possible to those that will occur at the 10^{35} $\text{cm}^{-2}\text{s}^{-1}$ luminosity (sLHC). To reach this goal we performed measurements with HEC, EMEC, and FCAL test modules using a high intensity (up to 10^{12} pps) beam of the IHEP (Protvino) 70 GeV accelerator.

FCAL, EMEC and HEC mini-modules

The ATLAS Forward Calorimeter (FCAL) will be exposed to the highest radiation doses. The part of the FCAL most affected is in the FCal1 module at smallest angles to the beam and at a depth near electromagnetic shower maximum. A small reproduction of the ATLAS Forward Calorimeter is housed in the first cryostat (see Fig. 2). As in ATLAS, the electrodes are composed of copper rods (anodes) within thin-walled copper tubes (cathodes). The rods in the sixteen tube/rod electrodes with 0.27 mm gaps are held at HV potentials up to +250V relative to the tubes while the rods in the sixteen tube/rod electrodes with 0.10 mm gaps are held at HV potentials up to +100 V relative to the tubes and copper matrix. Special features of the FCAL are internal nitrogen cooling loops near the periphery to remove heat generated in the module by the intense proton beam.

The EMEC module consists of four lead absorbers (2 mm Pb + 2 x 0.1 mm stainless steel) and three thin polyimide electrodes with 2 mm gaps between the electrodes and absorbers. The lateral size of the electrodes is 70 x 70 mm. The electrodes have three conductive layers, the positive HV (2 kV) is applied to the two outer layers, the signal is read out from the middle layer. The signal electrode is structured in four pads yielding four read-out channels in total.

The HEC module design follows closely the ATLAS HEC1 calorimeter: the thickness of the copper absorber plates is 25 mm, with the front plate 12.5 mm only. In total five absorber plates, yielding four liquid argon gaps, correspond to half of the first longitudinal section in ATLAS. The lateral size is 60 x 60 mm. Spacers define the 8.5 mm gaps between the absorber plates. The read-out structure follows the principle of an electrostatic transformer (EST). The EST and PAD electrodes correspond exactly to the ATLAS design, as well as the hexcel spacer mats and the signal and HV connections via strip-line polyimide connectors.

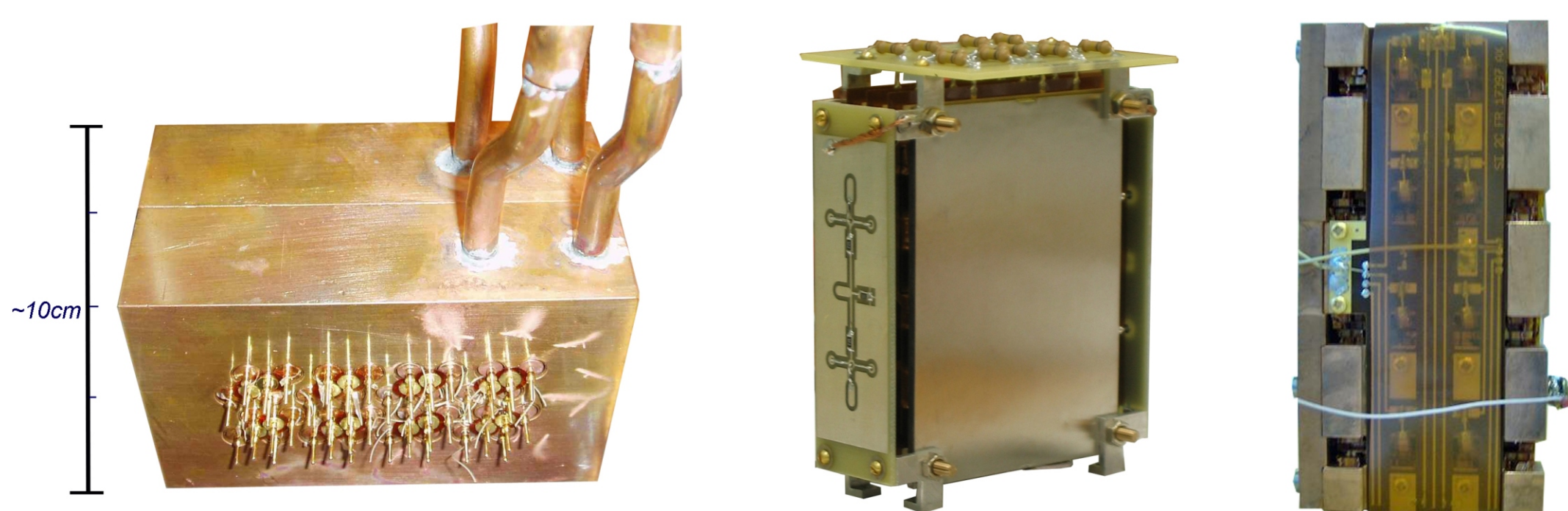


Fig. 1. FCAL, EMEC and HEC mini-modules respectively.

Each cryostat has been equipped with an impurity measuring device, which has been developed originally for the ATLAS experiment. The purity monitors consist of a combined ^{241}Am and ^{207}Bi monitor. These two sources provide 5 MeV α -particles and 1 MeV conversion electrons, respectively. For a short period of the November 2008 run the purity starting at a level of about 0.38 ppm deteriorates at a rate of ~ 23 ppb per day. But the impurity stays well below the limits needed for measurements, although a slight degradation can be observed.

Monitoring the temperature is not only crucial for the operation of the cryogenic system but also of interest in order to detect any increase of the cryostat and calorimeter module temperature due to a high particle flux. Four temperature probes of the PT-100 type have been installed in each of the three cryostats. The energy deposition at beam intensity of $5 \cdot 10^{11}$ pps (corresponding to luminosity $3 \cdot 10^{36}$ $\text{cm}^{-2}\text{s}^{-1}$) leads to increase of FCAL module temperature at the level of $\sim 0.5\text{K}$.

Beam set-up

The set-up of the three cryostats in the beam-line 23 at IHEP is shown in Figure 2. Each calorimeter module is in a separate cryostat and each cryostat is on a platform movable perpendicularly to the beam axis. Additional absorbers are placed in front and behind the FCAL cryostat. The position and thickness of the absorbers has been optimized in the MC simulation studies. Three scintillation counters in the beam line monitor the beam intensity in case of low intensity running, i.e. up to 10^7 pps. Similarly, a scintillation counter hodoscope with 16 horizontal and 16 vertical strips monitored the beam profile for these intensities. For higher intensity running three scintillation counters have been installed at an angle of about 45 degrees with respect to the beam. For intensities up to $1 \cdot 10^{11}$ pps a low pressure ionization chamber served as beam profile monitor. The correlation between the rate measured in the scintillation counters and the rate measured in the ionization chamber has proven to be linear within the beam intensity covered in the range $10^7 - 10^{10}$ pps. Since the November 2008 run the Cherenkov counter has been installed for monitoring the beam intensity bunch by bunch.

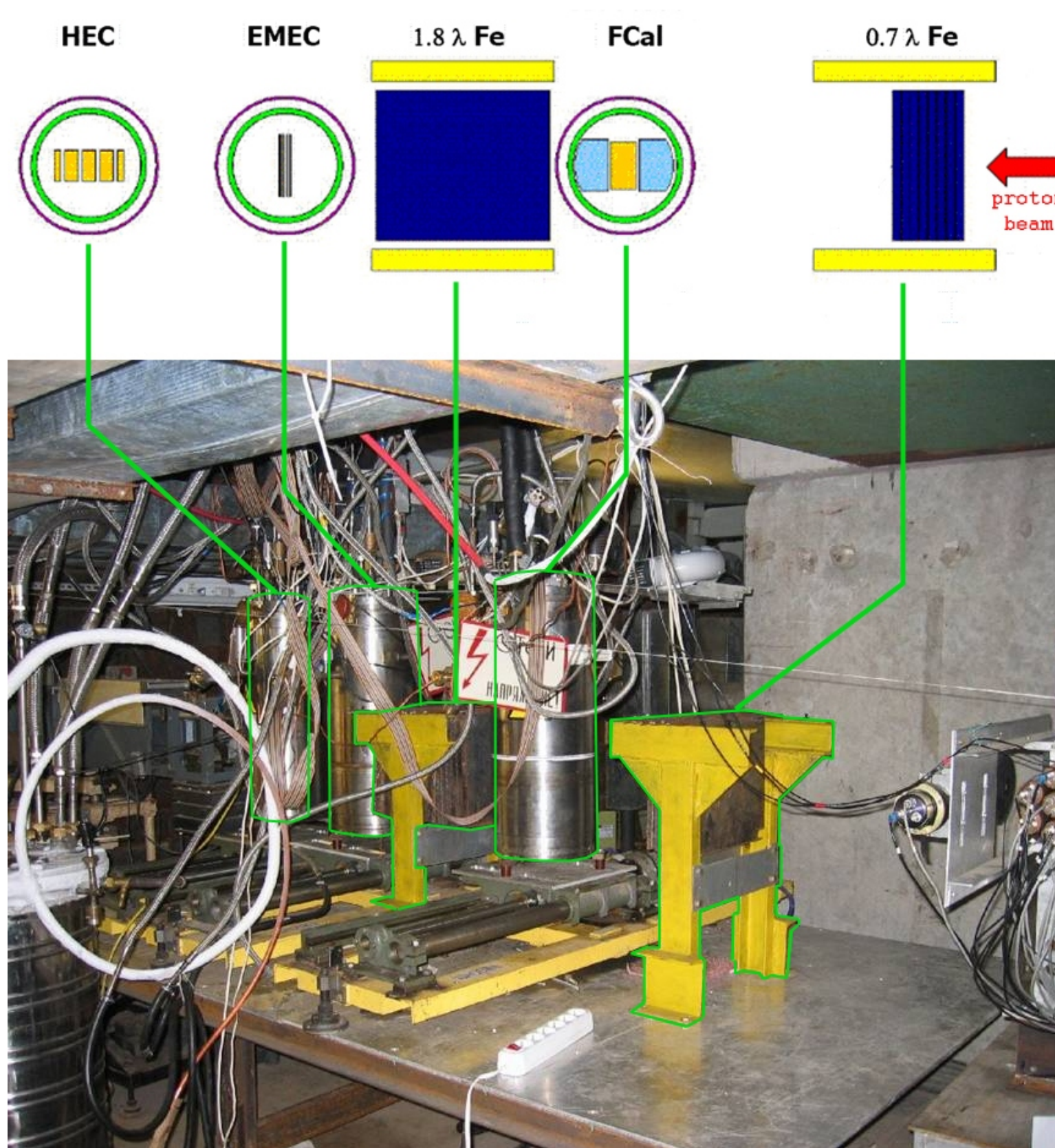


Fig. 2. Set-up of the FCAL, EMEC and HEC cryostats with calorimeter modules in the beam hall at IHEP (Protvino).

There are four read-out channels for the EMEC and HEC module and eight for the FCAL module (four for the FCAL with 0.27 mm gaps and four for the FCAL with 0.10 mm gaps). Channels are read-out by a front-end board (FEB) located 3 m away from the cryostats. Each calorimeter channel is connected to a 0T preamplifier and RC2-CR shaper with 15 ns time constant. The shaper has two outputs with low gain and medium gain. The gain ratio for these two outputs is about 10. Each shaper output is split into two drivers sending signals to two independent digitizers through a 35 m long differential line. The data acquisition system (DAQ) is based on the 32-channel 40 MHz flash ADC boards, storing up to 256 samples of the input data from the FEB (calorimeter and scintillator signals). Further components are the calibration board generating the pulses for the electronic calibration and modules to control and record the trigger and timing.

Data and preliminary results

In the last two run periods (2007-2008) data have been taken in the intensity range from $2 \cdot 10^7$ pps to $2 \cdot 10^{11}$ pps. The IHEP accelerator was running with only 5 filled bunches per turn in comparison to 30 bunches as used in the normal running mode. The (filled) bunch spacing was thus typically 990 ns, the bunch width about 15 ns FWHM. At low intensity the current due to the calorimeter response has a triangular shape with the length given by the drift time for the related liquid argon gap (for HEC with the nominal HV of 1.8 kV this corresponds to typically 450 ns). This signal is passed through an amplifier and shaper, yielding a typical peaking time of ~ 50 ns. For each event at least 64 time slice samples (spaced by 25 ns) have been read-out, covering thus the full history in time for the response of 2 filled bunches. When the rate is increasing the current shape is changing due to build-up of slowly drifting positive ions. The detailed theoretical study of this effect was performed in NIM A 482 (2002)156-178. For each module and HV setting a critical ionization rate D_c can be defined, where the charge build-up in the liquid argon gap is equal to the charge on the electrodes.

The Figure 3 shows the mean normalized HEC signal (sum of the four channels) for various beam intensities, varying from $2 \cdot 10^7$ pps up to $1.8 \cdot 10^{11}$ pps. For each event the signal has been fitted with a standard signal shape near the peak, with the peak time and the peak amplitude as free parameters. At higher fluxes the beam intensity varied stronger from bunch to bunch. This reflects in a wider variation of the signal amplitudes within a given beam intensity run. Therefore the mean normalized signal is shown (different colours) for different signal amplitudes. The intensity $3 \cdot 10^8$ pps is corresponding to the sLHC luminosity of 10^{35} $\text{cm}^{-2}\text{s}^{-1}$ at HEC. At low intensities the effects of the ion build-up are negligible. The current pulse has a triangular shape, the linear fall of the pulse after shaping causes a flat, negative signal response. With increasing beam intensity the current pulse is changing: the falling edge is shorter and sags, producing shorter and deeper negative signal after shaping. This decrease of the pulse length with beam intensity is evidently seen.

Figure 4 shows the mean signal amplitude for the four HEC channels for different beam intensities. Above a beam intensity of 10^{10} pps the nonlinearity of the response starts to get visible.

A charged particle passing the LAr gaps of the detector and producing drifting ions and electrons induces not only a signal in the read-out chain but also a DC current in the HV system. This current can be correlated with the average beam intensity, respectively the luminosity at LHC or sLHC. The measured currents were integrated over one spill for each channel separately. The data were compared with the beam intensity measured by the ionisation chamber on a spill by spill basis. This setup was used for beam intensities between 10^8 pps and 10^{11} pps simulating a particle flux through the calorimeter corresponding to 10^{33} $\text{cm}^{-2}\text{s}^{-1}$ + 10^{36} $\text{cm}^{-2}\text{s}^{-1}$ luminosity at the LHC. For this comparison a constant beam position relative to the cryostat was required. The corresponding measurements of the HV currents are shown in Figure 5 as a function of beam intensity as determined by the ionisation chamber. A polynomial of second order was used to account for residual non-linearities. The final result, when combining all 0.27 mm FCAL channels, shows a very good linear dependence between the FCAL HV current and the beam intensity, with a non-linearity of less than 0.36% (95% CL). This value is calculated for the nominal LHC luminosity of 10^{34} $\text{cm}^{-2}\text{s}^{-1}$, corresponding here to 10^9 pps. Taking beam position variations into account a precision for relative luminosity measurement in ATLAS of 0.5% is expected using this measurement.

Conclusion

Some new important results concerning the operation of the ATLAS liquid argon end-cap calorimeters at high luminosities have been obtained. The signal shape changing was observed at high intensities. The correlation between beam intensity and read-out signal has been studied. Also dependence of the HV currents as well as calorimeter module temperature on the beam intensity has been measured. After analysis of the already collected data and the data which will be collected in the next run we hope to establish operating limits of the ATLAS liquid argon end-cap calorimeters at luminosity of 10^{35} $\text{cm}^{-2}\text{s}^{-1}$ by the following detailed studies:

1. Studies of calorimeter cell response as a function of beam intensity and HV applied to the cell.
2. Measurement of argon purity versus integrated particle flux.
3. Measurement of the radioactive pollution of liquid argon, calorimeter components and materials as a function of integrated particle flux.
4. Analysis of the signal shapes as function of integrated particle flux.

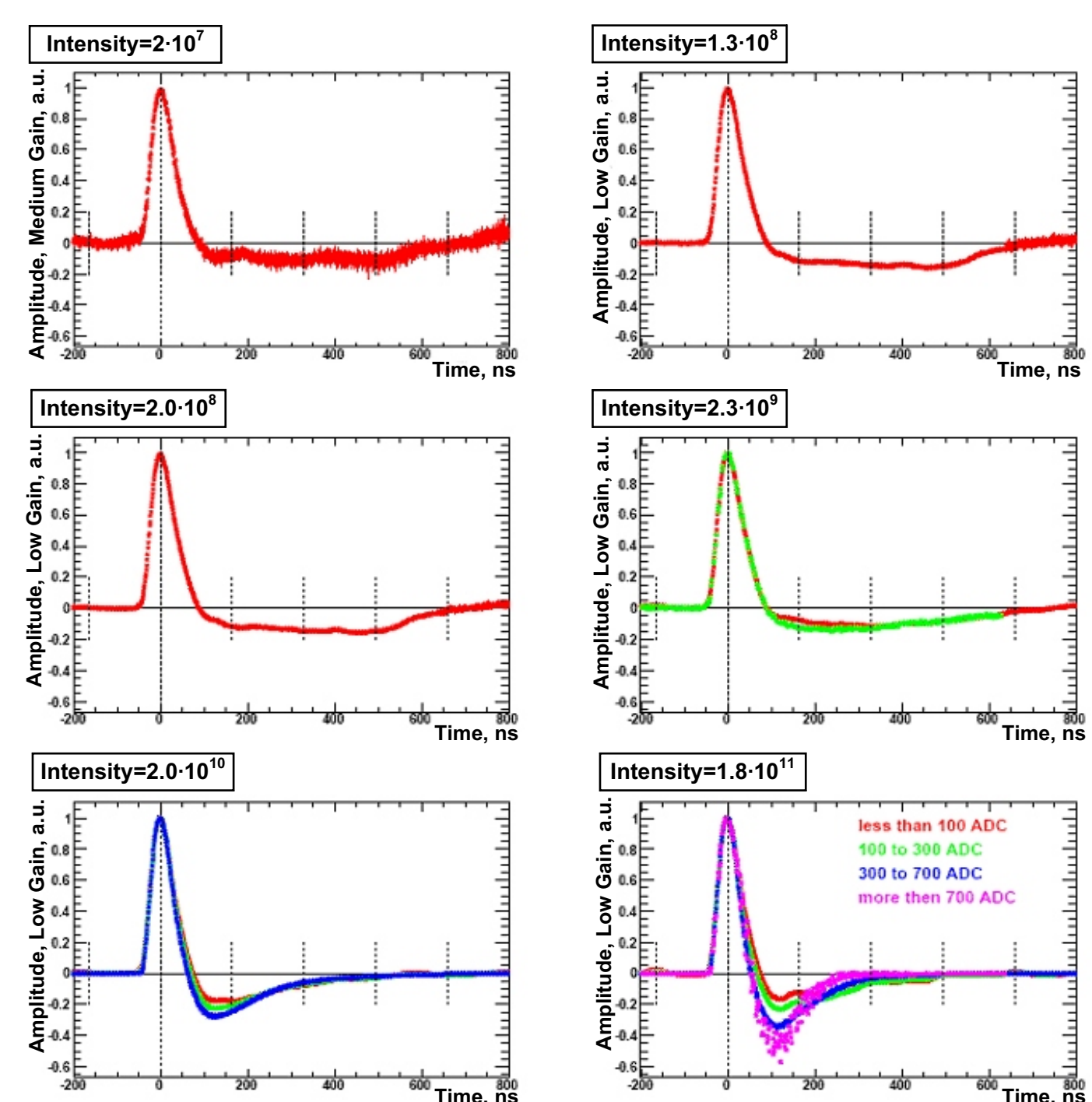


Fig. 3. Normalized HEC signal for various beam intensities, varying from $2 \cdot 10^7$ pps up to $1.8 \cdot 10^{11}$ pps. The mean normalized signal is shown (different colours) for different signal amplitudes. Critical ionization rate D_c corresponds to $8 \cdot 10^8$ pps.

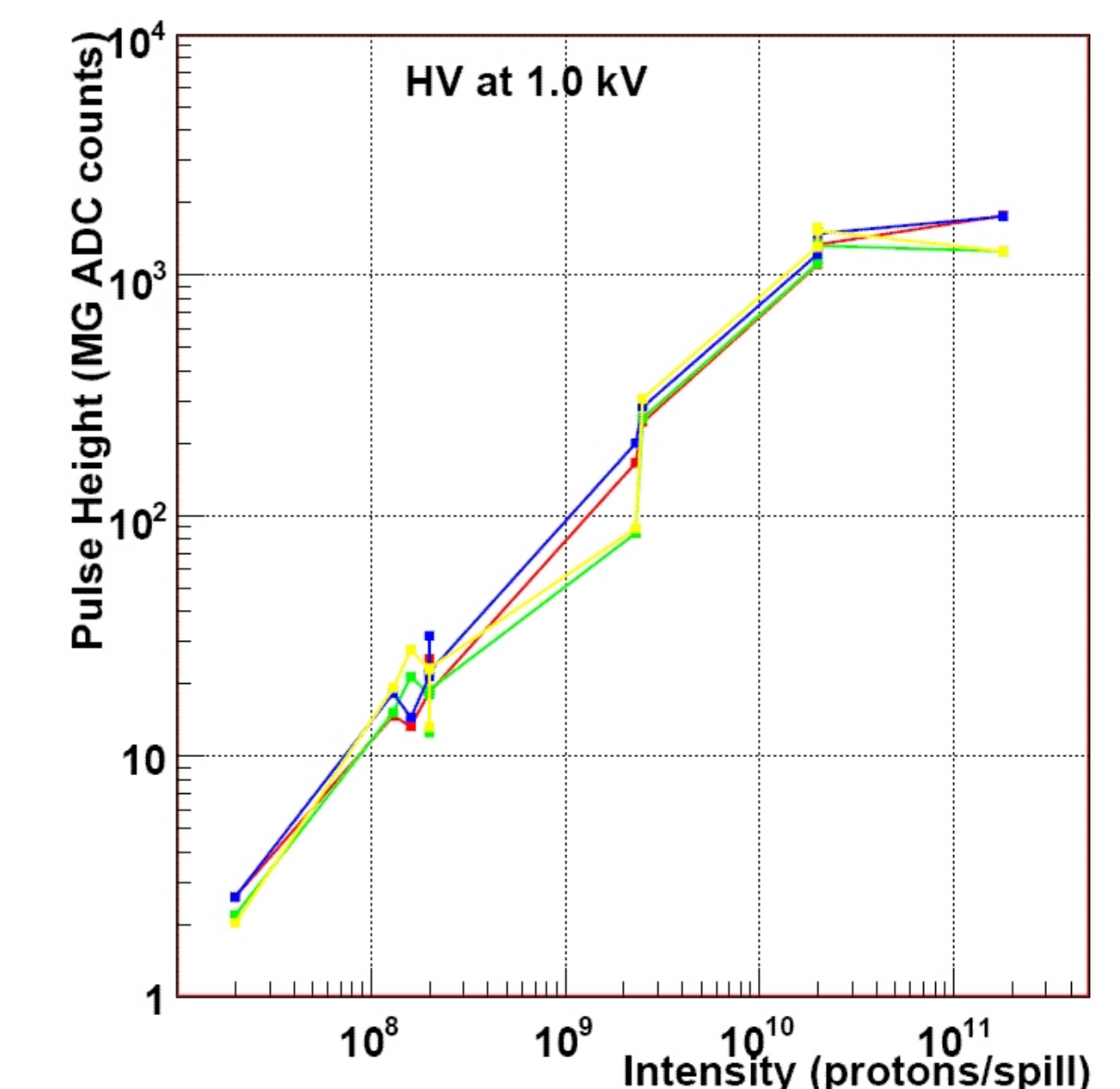


Fig. 4. Mean signal amplitude for the four HEC channels for different beam intensities.

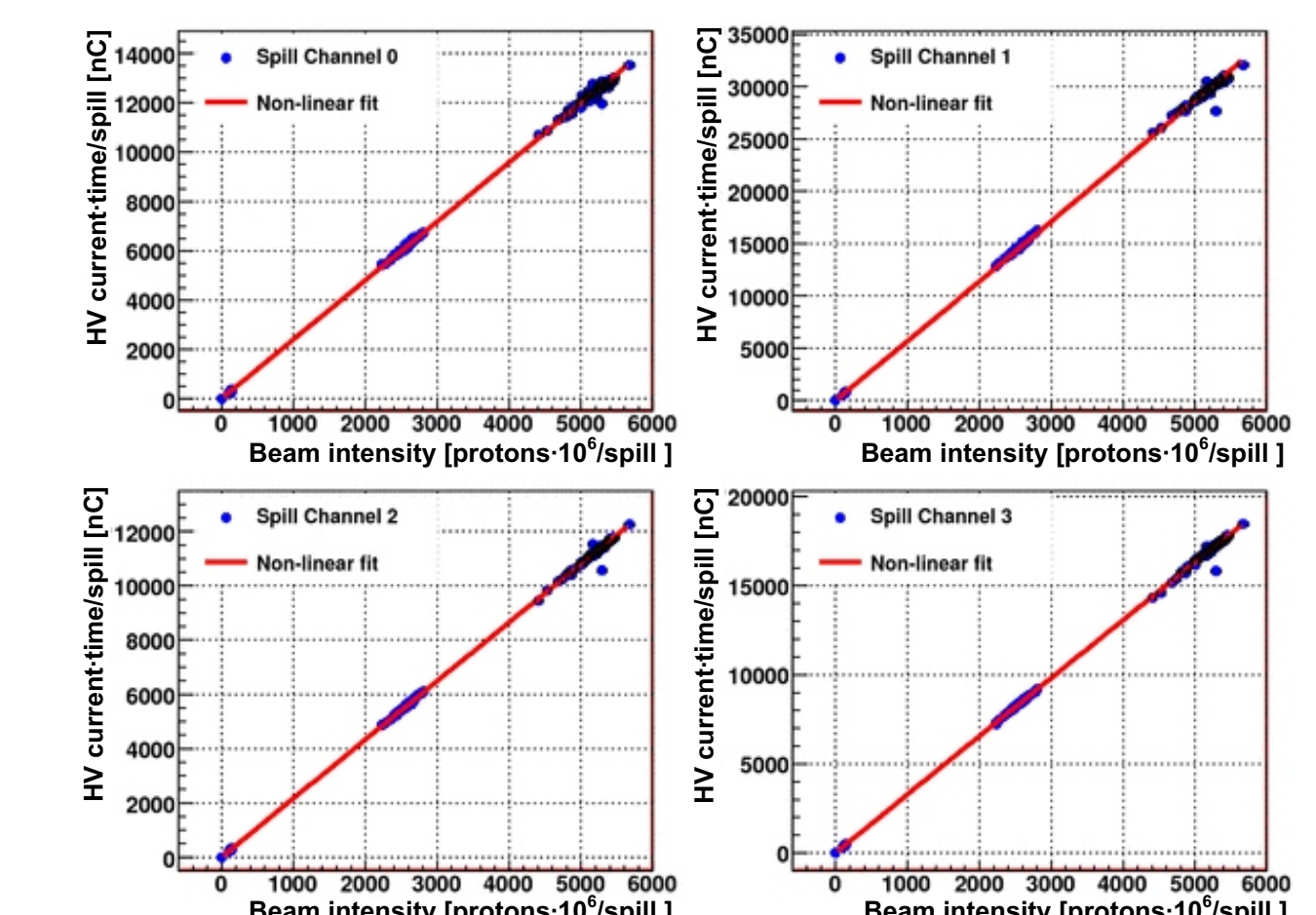


Fig. 5. FCAL HV current measurement vs. beam intensity.